0026-895X/05/6706-1909–1919$20.00
MOLECULAR PHARMACOLOGY
Copyright © 2005 The American Society for Pharmacology and Experimental Therapeutics
Mol Pharmacol 67:1909–1919, 2005

Vol. 67, No. 6
10165/3033314
Printed in U.S.A.

Endoplasmic Reticulum Stress Links Dyslipidemia to Inhibition of Proteasome Activity and Glucose Transport by HIV Protease Inhibitors

Rex A. Parker, Oliver P. Flint, Ruth Mulvey, Carolina Elosua, Faye Wang, William Fenderson, Shulin Wang, Wen-Pin Yang, and Mustafa A. Noor

Metabolic and Cardiovascular Discovery Biology (R.A.P., S.W.), Discovery Toxicology (O.P.F., R.M., C.E., F.W.), Applied Genomics (W.F., W.-P.Y.), and Virology Medical Affairs (M.A.N.), Bristol-Myers Squibb Pharmaceutical Research Institute, Pennington, New Jersey

Received December 8, 2004; accepted March 8, 2005

ABSTRACT

The lipid and metabolic disturbances associated with human immunodeficiency virus (HIV) protease inhibitor therapy in AIDS have stimulated interest in developing new agents that minimize these side effects in the clinic. The underlying explanation of mechanism remains enigmatic, but a recently described link between endoplasmic reticulum (ER) stress and dysregulation of lipid metabolism suggests a provocative integration of existing and emerging data. We provide new evidence from in vitro models indicating that proteasome inhibition and differential glucose transport blockade by protease inhibitors are proximal events eliciting an ER stress transcriptional response that can regulate lipogenic pathways in hepatocytes or adipocytes. Proteasome activity was inhibited in vitro by several protease inhibitors at clinically relevant (micromolar) levels. In the intact cells, protease inhibitors rapidly elicited a pattern of gene expression diagnostic of intracellular proteasome inhibition and activation of an ER stress response. This included induction of transcription factors GADD153, ATF4, and ATF3; amino acid metabolic enzymes; proteasome components; and certain ER chaperones. In hepatocyte lines, the ER stress response was closely linked to moderate increases in lipogenic and cholesterogenic gene expression. However, in adipocytes where GLUT4 was directly inhibited by some protease inhibitors, time-dependent suppression of lipogenic genes and triglyceride synthesis was observed in coordination with the ER stress response. These results further link ER stress to dyslipidemia and contribute to a unifying mechanism for the pathophysiology of protease inhibitor-associated lipodystrophy, helping explain differences in clinical metabolic profiles among protease inhibitors.

The development and clinical use of HIV protease inhibitors have contributed greatly to treatment of HIV-AIDS as a critical component of highly active antiretroviral therapy (HAART) regimens. With this efficacy has come recognition of an associated syndrome of metabolic side effects that is relevant in evaluating the long-term risk/benefit of treatment options (Calza et al., 2004). The constellation of metabolic problems with protease inhibitors includes hyperlipidemia, insulin resistance, peripheral lipoatrophy, central fat accumulation, and hepatic steatosis. Despite several hypotheses to explain clinical findings, the cellular and molecular mechanisms underlying this lipodystrophy-like syndrome are incompletely understood. Recent clinical studies in patients (Woerle et al., 2003; Calza et al., 2004) and in normal subjects (Purnell et al., 2000; Noor et al., 2002, 2004) have confirmed a direct connection between some protease inhibitors and metabolic effects, despite the complexity of multidrug therapy and virological and immunological responses during HAART. The recent emergence of a newer generation of protease inhibitor that exhibits antiviral efficacy without adverse affects on lipid or glucose parameters in the clinic (Haas et al., 2003; Murphy et al., 2003; Sanne et al., 2003; Cahn et al., 2004; Noor et al., 2004; Squires et al., 2004) provided an opportunity to reexamine the molecular pharmacology and toxicology of the protease inhibitor class.

Article, publication date, and citation information can be found at http://molpharm.aspetjournals.org.
doi:10.1124/mol.104.010165.

ABBREVIATIONS: HIV, human immunodeficiency virus; HAART, highly active antiretroviral therapy; GLUT, glucose transporter; SREBP, sterol regulatory element binding protein; ER, endoplasmic reticulum; UPR, unfolded protein response; DMSO, dimethyl sulfoxide; suc-LLVY-amc, succinyl-Leu-Leu-Val-Tyr-7-amino-4-methylcoumarin; FPLC, fast-performance liquid chromatography; RT-PCR, real-time polymerase chain reaction; hsp/HSP, heat shock protein; C/EBP homologous protein; GADD, growth arrest and DNA-damage inducible; ATF, activating transcription factor; MG132, *N*-benzoyloxycarbonyl (*Z*)-Leu-Leu-leucinal; PEPCK, phosphoenolpyruvate carboxykinase; FAS, fatty acid synthase; PPAR, peroxisome proliferator-activated receptor.

Previous studies revealed that protease inhibitors interfere with key intracellular processes regulating glucose and lipid metabolism in major insulin-responsive tissues. Several protease inhibitors directly inhibit glucose transporter activity in adipocytes, in particular glucose transporter (GLUT)4, which is essential for normal insulin-responsive glucose uptake in adipose and muscle (Murata et al., 2000; Hruz et al., 2001; Hertel et al., 2004). Differential inhibition of GLUT4 is believed to explain differences between HIV protease inhibitors on insulin-stimulated glucose disposal in clinical studies using the euglycemic hyperinsulinemic clamp technique (Noor et al., 2002, 2004).

Protease inhibitors also seem to influence lipid and cholesterol metabolism by inhibiting the degradation of the key transcription factors that control lipid pathways, the sterol regulatory element binding proteins (SREBPs). Degradation of nuclear SREBPs by the proteasome was directly demonstrated in mammalian cells (Hirano et al., 2001), and proteasome activity was unexpectedly shown to be inhibited by some HIV protease inhibitors in vitro (Schmidtke et al., 1999; Pajonk et al., 2002). However, effects of HIV protease inhibitors on SREBP levels and translocation and on SREBP-targeted lipogenic gene expression in liver and adipose tissue have proven to be complex (Dowell et al., 2000; Caron et al., 2003; Hui, 2003). Further insight into the role of proteasome came from studies showing that processing of apolipoprotein B by proteasome activity in hepatocytes is perturbed by HIV protease inhibitor treatment in HepG2 cells (Liang et al., 2001), which could contribute to dyslipidemia.

Interference with proteasome function could underlie the lipid effects of protease inhibitors to a greater extent than previously suggested. The surveillance function of proteasome coordinates protein synthesis, folding, and trafficking in the endoplasmic reticulum (ER), and its disruption triggers an adaptive mechanism termed the unfolded protein response (UPR) or more generally the ER stress response. This includes activation of transcription factors and downstream effectors, including ER chaperones and amino acid and protein metabolic enzymes (Travers et al., 2000; Kaufman et al., 2002). Other physiological factors, notably glucose or nutrient deprivation, influence ER stress and affect the scope and extent of the transcriptional response (Kaufman et al., 2002). It was reported recently that ER stress is exacerbated by intracellular lipid deposition and that obesity and metabolic disturbances are closely linked to ER stress and its consequences in both adipose tissue and liver (Ozcan et al., 2004).

The topology and localization of lipid synthetic enzymes in the ER suggested that further investigation of the relationship between the ER stress response and lipogenesis could provide new insights into protease inhibitor-associated lipid disorders. As first described in preliminary reports (Parker et al., 2003), these studies revealed a deeper mechanistic link between cellular adaptive responses to protease inhibitors and the transcriptional regulation of lipid metabolism in adipocytes and hepatocytes. The results of these experiments contribute to an integrated mechanism extending previous hypotheses and help to explain the differences in metabolic profiles observed among the HIV protease inhibitors in clinical use.

Materials and Methods

Cell Culture. HepG2 cells (human hepatoma cell line), TC5 cells (human transformed normal hepatocyte line), and 3T3-L1 adipocytes (mouse preadipocytes differentiated to mature fat cells by standard protocols for 5 days before studies) were treated for 24 h or for the time courses indicated with HIV protease inhibitors at the indicated concentrations in culture media containing 10% fetal bovine serum. Primary rat adipocytes from normal male Wistar rats were obtained by standard collagenase isolation technique and incubated in Krebs-Ringer-HEPES buffer with 2% albumin.

Biochemicals. Protease inhibitors lopinavir, nelfinavir, ritonavir, and saquinavir were purified by reverse phase high-performance liquid chromatography from commercial pharmaceutical preparations. Atazanavir was provided in pure form by Bristol-Myers Squibb Chemistry Division. Purified protease inhibitors and stock solutions in DMSO were stored at −20°C. Drugs stocks in DMSO were diluted into culture media containing bovine serum or albumin to aid solubility and sterile filtered before use. Solutions were monitored microscopically to avoid possible precipitation of drugs. Vehicle control incubations received the same final DMSO concentration as all drug-treated incubations (0.1%). Proteasome fluorogenic peptide substrates succinyl-Leu-Leu-Val-Tyr-7-amino-4-methylcoumarin (suc-LLVY-amc) and *N-tert*-butoxycarbonyl-LRR-7-amino-4-methylcoumarin were obtained from Bachem Biosciences (King of Prussia, PA), and human 20S proteasome preparation was obtained from Chemicon International (Temecula, CA).

Lipid Biosynthesis. Triglyceride and cholesterol synthesis were assayed in cells by incorporation of 1 μCi/ml 2-[^{14}C]acetate over the final 3 h of 24-h incubations with protease inhibitors or times indicated. Lipids were extracted from cells in organic solvents and separated by planar chromatography followed by determination of radioactivity by microarray channel detector (Instant Imager, PerkinElmer Life and Analytical Sciences, Boston, MA).

GLUT Assay. 3T3-L1 adipocytes were incubated with protease inhibitors in Krebs-Ringer-HEPES buffer with 2% fetal bovine serum for 30 min, followed by addition of 1 μM insulin for 20 min, and then GLUT activity was assayed as uptake of [^{3}H]2-deoxyglucose for 10 min essentially as described previously (Murata et al., 2000). Primary adipocytes followed the same protocol except that the buffer was supplemented with 2% albumin.

FPLC Superose-6 Isolation and Assay of Proteasome Activity. Native proteasome fractions were prepared from cultures of HepG2 cells and 3T3-L1 cells (as undifferentiated preadipocytes) following the method of Rodgers and Dean (2003), briefly as follows. Cells grown in 225-cm^2 flasks were harvested at 80 to 90% confluence, and cells were lysed by shaking for 30 min at 4°C in 20 mM Tris-HCl, pH 7.5, with 10% glycerol, 5 mM ATP, and 0.2% Nonidet P-40 (buffer A). Lysates were centrifuged at 10,000*g* for 10 min, and the supernatant was collected and concentrated 10-fold in Centricon Plus-20 centrifuge filters (100-kDa molecular mass cut-off), followed freezing at −80°C. Aliquots (150 μl) of once-thawed concentrates were chromatographed by gel filtration on an AKTA FPLC system using Superose-6 gel filtration in buffer A at 0.50 ml/min, and fractions of 300 μl were collected at 20°C. For the assay of proteasome activity, 10-μl aliquots of each FPLC fraction were incubated in 96-well plates containing 20 mM Tris-HCl, pH 7.5, with or without respective inhibitors added with mixing to provide final concentrations indicated in figures, and a final DMSO level of 0.1%, in a total volume of 100 μl. The enzyme assay was then initiated by addition of the fluorogenic protease substrate suc-LLVY-amc at 50 μM (final), mixing, and incubation at 37°C for 45 min, followed by determination of amc product fluorescence in a Cytofluor-2 plate reader at 380 excitation/460 emission. Product formation was linearly proportional to time and enzyme concentration. Proteasome activity units are defined as relative fluorescence of LLVY-amc product per assay under these conditions. Purified human erythrocyte 20S proteasome preparations were obtained from Chemicon International. Aliquots

of 20S proteasome were incubated with protease inhibitors in vitro, followed by the assay of chymotryptic proteolytic activity using the fluorogenic substrate suc-LLVY-amc as described above and essentially according to Schmidtke et al. (1999). Reaction rates were determined over a 30-min incubation period, and percentage of inhibition was calculated.

RNA Isolation. Total cellular RNA was isolated from cultured HepG2, TC5, and 3T3-L1 cells, using the standard QIAGEN (Valencia, CA) method, including treatment with DNase. cDNA and cRNA were generated from the cellular RNA using Invitrogen (Carlsbad, CA) and Enzo Diagnostics (New York, NY) methods for gene expression profiles and real-time polymerase chain reaction (RT-PCR).

Transcriptional Profiling. Affymetrix gene profiling (human U133A chips, with 22,214 total RNA sequences profiled; and murine U74Av2 chips with 12,422 RNA sequences) was conducted to assess gene expression. RNA samples were isolated from triplicate cell incubation samples (HepG2) or from duplicate cell incubation samples repeated twice (adipocytes). Affymetrix-recommended protocol was used in the generation of cRNA probe and hybridization of chips. Suite version 5.0 was used to scan and quantitate the chip. Data were evaluated for Affymetrix P call, average change in expression (ratio of mean drug-treated/mean control), and significance of difference between drug treated and control was determined by t test ($p < 0.01$ taken as significant). Results for key genes were confirmed by RT-PCR.

RT-PCR. To confirm and extend the transcription profiles, mRNA for selected genes was assayed by RT-PCR in RNA samples taken from independent experiments using cell incubation time courses. SYBR green RT-PCR protocols were used to assay relative changes in gene expression, quantitated by the ΔΔCT method, and mRNA values for each gene were normalized to internal control cyclophilin B mRNA. The ratio of normalized mean value for drug-treated groups to vehicle control was calculated and is given in the graphs.

Results

Proteasome Inhibition by HIV Protease Inhibitors. Five HIV protease inhibitors currently in clinical use were assayed for inhibition of proteolytic cleavage activity in purified human 20S proteasome samples. Concentration-dependent inhibition of chymotryptic activity was observed at levels >1 μM for several of the protease inhibitors (Fig. 1A). The rank order and IC_{50} values for 20S proteasome inhibition were saquinavir (IC_{50} = 3 μM), nelfinavir (4 μM), lopinavir (9 μM), ritonavir (11 μM), and atazanavir (26 μM). A procedure to isolate and assay 26S/20S proteasome from mammalian cells described previously (Rodgers and Dean, 2003) was adapted to assay the high molecular weight proteolytic activity in FPLC Superose-6 gel filtration fractions isolated from 3T3-L1 and HepG2 cell lysates (Fig. 1B). The lactacystin-inhibitable fractions were pooled and concentrated and used as the sources of 26S/20S proteasome to assay the effects of HIV protease inhibitors on the hydrolysis of chymotryptic and tryptic fluorogenic peptide substrates. In proteasome preparations from both cell types, lactacystin inhibited chymotryptic activity potently ($IC_{50} < 1$ μM) and tryptic activity moderately (IC_{50} ~20 μM), whereas MG132 strongly inhibited the tryptic activity ($IC_{50} < 1$ μM) (Fig. 1C), consistent with the properties of these well characterized, high-affinity proteasome inhibitors (Zimmermann et al., 2000; Rodgers and Dean, 2003). In comparison with these controls, the HIV protease inhibitors moderately inhibited proteasome chymotryptic activity at micromolar levels in the HepG2 and 3T3-L1 preparations, with modest differences between compounds observed (Fig. 1C). Weaker inhibition of tryptic activity was also observed under these conditions (Fig. 1C).

Effects of Protease Inhibitors on Lipogenesis and Glucose Transport in Adipocyte and Hepatocyte Models. Before incubation with protease inhibitors, 3T3-L1 adipocytes were first differentiated for 5 days to reach a distinct lipid storage droplet morphology with an avid triglyceride biosynthesis rate. Under these conditions, exposure to HIV protease inhibitors at micromolar concentrations for 24 h suppressed adipocyte triglyceride synthesis, assayed as the incorporation of [^{14}C]acetate precursor at the end of the incubation (Fig. 2A). Varying potencies were observed for the five protease inhibitors tested. In time-course studies (up to 48 h), the decrease in cellular lipid biosynthesis was time-dependent with greatest effect at 24-h incubation (Fig. 2B). Under these conditions, protease inhibitors did not affect cellular ATP levels, suggesting that they were not cytotoxic.

In adipose tissue, glucose uptake is required for glycolysis, yielding energy and lactate as well as provision of glycerol-3-phosphate (through the action of glycerol-3-phosphate dehydrogenase on dihydroxyacetone phosphate) essential as precursor for the triglyceride backbone. In 3T3-L1 adipocytes under conditions similar to those used to assay lipogenesis, the protease inhibitors acutely inhibited 2-deoxyglucose uptake assayed in the presence of insulin, with different magnitudes of glucose transport inhibition seen with each protease inhibitor (Fig. 2C). The 3T3-L1 cells under these conditions expressed approximately equal levels of both GLUT4 and GLUT1 mRNA. To better evaluate GLUT4-dependent effects, additional studies were conducted using primary rat adipocytes that express relatively high levels of GLUT4. In the primary adipocytes, ritonavir acutely inhibited insulin-stimulated glucose transport to a level near the insulin-free control value (Fig. 2D). Lactate released into the medium by the adipocytes over a 6-h incubation was concomitantly inhibited by ritonavir in parallel incubations, whereas atazanavir was essentially without effect on either endpoint (Fig. 2D). These data demonstrate that protease inhibitors differentially inhibit GLUT4-mediated glucose uptake by adipocytes and limit the intracellular availability of glucose resulting in diminished formation of a glucose-derived metabolite, lactate.

In contrast to the suppression observed in adipocytes, in HepG2 cells protease inhibitors tended to increase lipogenesis. Triglyceride biosynthesis rate was elevated to varying degrees by the five compounds studied over 3 to 30 μM at 24 h, and 6 to 48 h at 10 μM (Fig. 2E). Cholesterol synthesis under the same conditions in HepG2 cells did not change or was modestly increased (up to 20% increase over control). No effect on cellular ATP levels was observed under these conditions, suggesting the lack of cytotoxicity. The increases in lipogenesis in HepG2 cells were observed at concentration ranges of the protease inhibitors that resulted in proteasome inhibition in vitro, although the apparent potencies in the two assays were only roughly correlated. Unlike the adipocytes, under conditions in which lipid synthesis was affected, glucose uptake was not significantly affected by any of the protease inhibitors studied in HepG2 cells. The lack of glucose transport inhibition is consistent with the finding that HepG2 cells express GLUT3 and GLUT1, which are relatively insensitive to inhibition by HIV protease inhibitors, but that do not express GLUT4, which is sensitive.

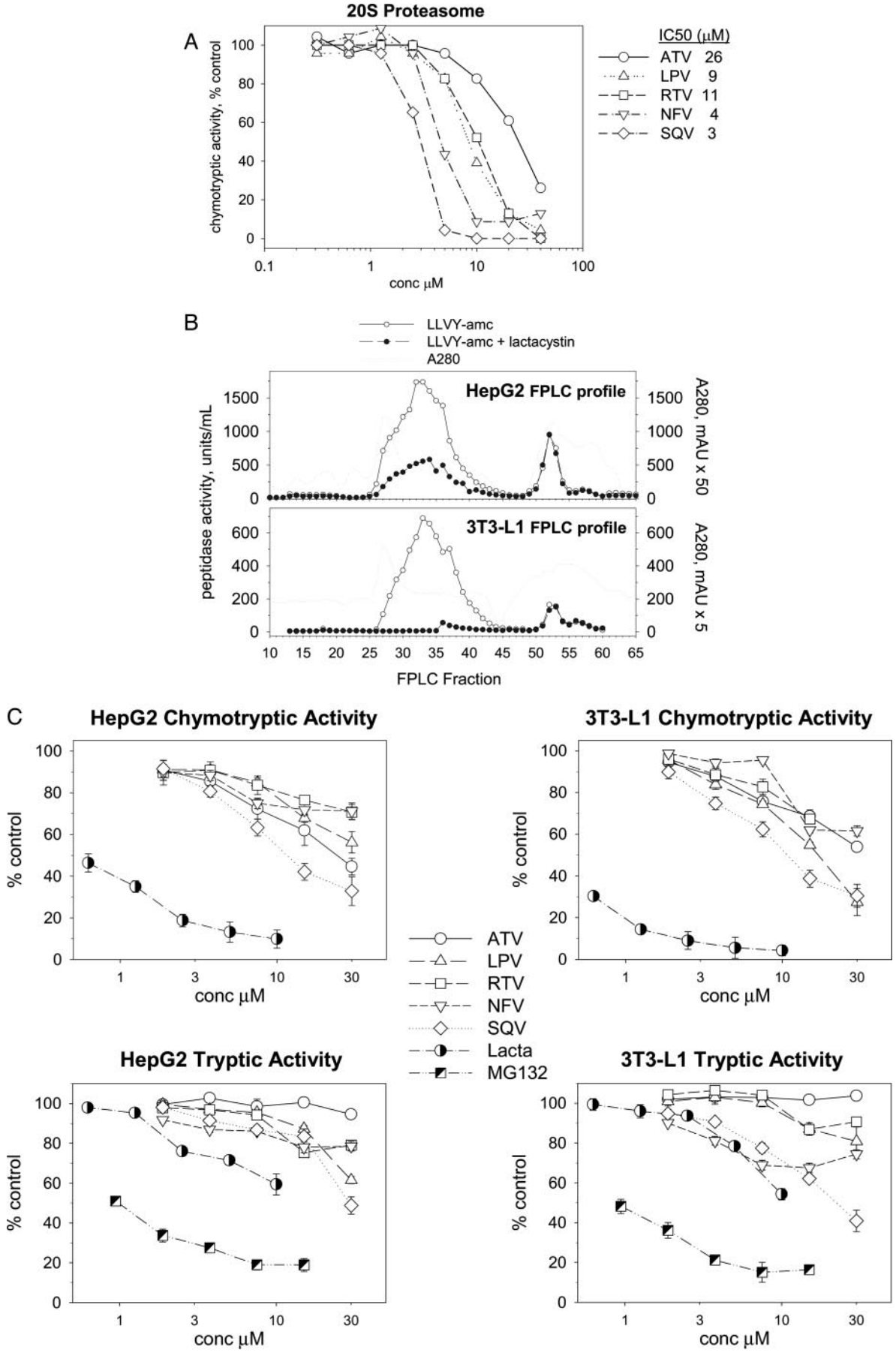

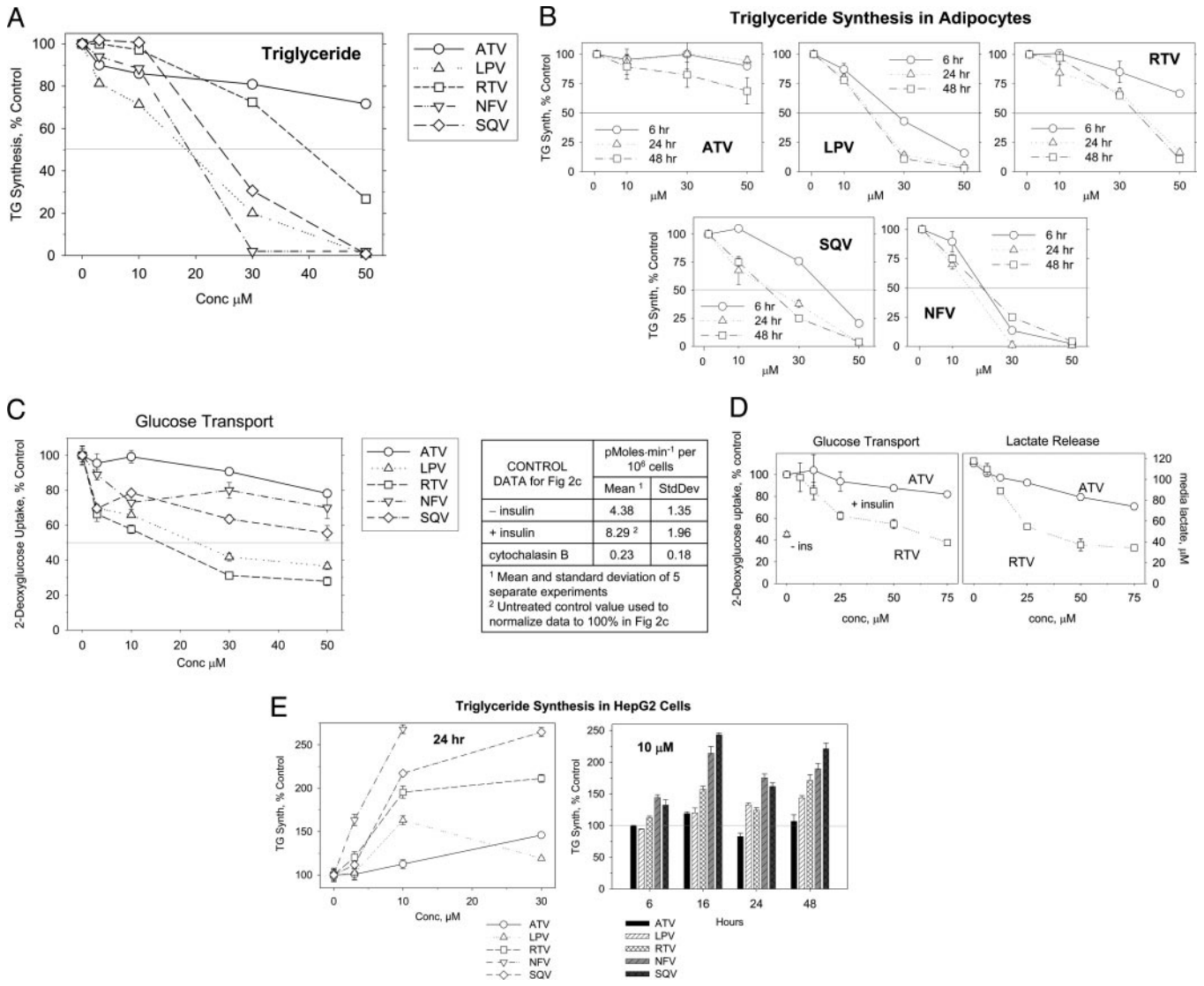

Fig. 2. Effects of protease inhibitors on metabolic functions in differentiated 3T3-L1 adipocytes and HepG2 cells. A, effects of protease inhibitors on lipid synthesis in 3T3-L1 adipocytes at end of 24-h incubation. The effect of each drug is indicated as percentage of control incorporation of [^{14}C]acetate into cellular triglyceride determined by quantitative analytical thin layer chromatography. Data are mean ± S.D. for triplicate cultures. B, time dependence of effect of protease inhibitors on triglyceride synthesis in 3T3-L1 adipocytes. Different symbols represent preoccupation times for each drug as indicated before assay of triglyceride synthesis. Data are mean ± S.D. for triplicate cultures. C, short-term effects of protease inhibitors on glucose uptake in differentiated 3T3-L1 adipocytes in the presence of insulin. Effect of each drug is indicated as mean percent of control transport of [^{3}H]2-deoxyglucose; text inset provides absolute rates. D, short-term effects of ritonavir and atazanavir on insulin-stimulated glucose transport in primary rat adipocytes, assayed as [^{3}H]2-deoxyglucose, and on lactate released into the medium over a 6-h incubation. E, effects of protease inhibitors on triglyceride synthesis in HepG2 Cells. Effect of each drug is indicated as percentage of control incorporation of [^{14}C]acetate into cellular triglyceride, for various concentrations of drug at 24 h (left), or at various times of treatment with 10 μM drug (right). Radiolabeled triglyceride was assayed by quantitative thin layer chromatography. Data are mean ± S.D. for four experiments. Drug abbreviations are as in Fig. 1.

Gene Expression Profiles in Hepatocyte and Adipocyte Models. Affymetrix gene expression profiling was conducted to further evaluate cellular and molecular adaptive responses to the effects of protease inhibitors. Cells were treated for 24 h with vehicle control or protease inhibitors under the conditions used in the functional assays, followed by mRNA isolation. Overall, less than 1% of the profiled RNA sequences increased or decreased by greater than 2-fold versus controls for any of the protease inhibitors tested (from a total of 22,214 and 12,422 total sequences analyzed for HepG2 cells and adipocytes, respectively). Of the genes significantly affected, approximately 4 times as many were in-

Fig. 1. Inhibition of proteasome activity in vitro by HIV protease inhibitors. A, inhibition of purified human 20S proteasome activity, assayed as cleavage of the fluorogenic peptide suc-LLVY-amc, given as mean percentage of inhibition versus control from triplicate assays for each concentration of protease inhibitor. B, chymotryptic (suc-LLVY-amc cleavage) activity in fractions from FPLC Superose-6 gel filtration chromatography of lysates from HepG2 and 3T3-L1 cells, assayed without and with the proteasome inhibitor lactacystin (1 μM). C, inhibition of proteasome activity by HIV protease inhibitors and reference compounds lactacystin (lacta) and MG132, assayed with FPLC Superose-6-derived 26S + 20S proteasome preparations from HepG2 and 3T3-L1 cells. Chymotryptic (suc-LLVY-amc) and tryptic (*N-tert*-butoxycarbonyl-Leu-Arg-Arg-7-amino-4-methylcoumarin) activities were assayed using fluorogenic peptide substrates. HIV protease inhibitors are abbreviated as follows: atazanavir, ATV; lopinavir, LPV; nelfinavir, NFV; ritonavir, RTV; and saquinavir, SQV.

duced than repressed in HepG2 cells (Fig. 3A). In comparison, an opposite general pattern emerged from the adipocytes, with more genes repressed than induced (Fig. 3B). Differences between the individual protease inhibitors were apparent (Fig. 3, A and B).

Detailed analysis of the expression profile in HepG2 cells revealed induction of several transcription factors that regulate expression of ER stress response components, including C/EBP homologous protein/GADD153, ATF4, CCAAT/EBP-β, CCAAT/EBP-γ, and the proteasome-interacting LIM-domain-only protein CSRP3e (Table 1). Multiple genes for amino acid biosynthesis and transport, amino acyl tRNA synthetases, glutathione metabolism, and chaperones such as the DnaJ/HSP40 homologs involved in the ER stress response were also induced (Table 1). Other genes involved in proteasome and ER function were also induced, including ubiquitin ligase, stanniocalcin-2, calmegin, and exportin T. Suppression of serum and glucocorticoid-regulated kinase, a regulator of the E3 ubiquitin-protein ligase (Nedd4-2) was observed. The magnitudes of change in ER stress and UPR gene expression in HepG2 cells were lower for atazanavir than the other protease inhibitors tested (Table 1).

Lipogenic Gene Expression in Coordination with ER Stress Response. The ER stress response to HIV protease inhibitors in HepG2 cells was associated with moderate but significant increases in mRNA encoding several enzymes of fatty acid and cholesterol biosynthesis pathways (Table 1). These included acetyl CoA carboxylase, fatty acyl CoA ligase, fatty acid synthase, diacylglycerol acyltransferase, HMGCoA reductase, mevalonate kinase, Nieman-Pick protein C1 (NPC1), and the low-density lipoprotein receptor. The gluconeogenic enzyme PEPCK, a known target of ATF4, was induced along with glucokinase regulatory protein (Table 1). The expression profile exhibited concentration dependence over the range of 3 to 10 μM (for nelfinavir) or 10 to 30 μM (for ritonavir and atazanavir) for several of these genes, similar to the concentration dependencies in the functional assays. It is interesting that expression of SREBP-1c and X-box binding protein-1 mRNA was not significantly affected by the protease inhibitors.

The Affymetrix transcription profile was confirmed and extended in separate experiments with HepG2 cells and the human hepatocyte TC5 cell line by quantitative RT-PCR. Coordinate induction of genes representing the ER stress response, amino acid homeostasis, and lipid/metabolic pathways were observed in time courses (Fig. 4A). Marked, rapid increases in mRNA for ATF4 (to 15-fold), GADD153 (to 12-fold), and C/EBP-β (to 6-fold) were observed for nelfinavir, ritonavir, and lopinavir in the hepatocyte cell line, whereas atazanavir-treated cells remained relatively quiescent over the 32-h time course (Fig. 4A). These changes were closely followed by induction of asparagine synthetase (up to >60-fold with nelfinavir), acetyl-coenzyme A carboxylase-α (to 4-fold with ritonavir), and PEPCK (to 25-fold with lopinavir).

Down-Regulation of Lipogenesis Genes in Adipocytes. The expression profile in adipocytes revealed induction of transcription factors and mediators of the ER stress response (ATF3, GADD153, ATF4, and GADD45), enzymes of amino acid, glutathione, and protein metabolism, and other components of the ER stress response, consistent with proteasome inhibition and the UPR (Table 2). However, in contrast to the hepatocyte models, the key lipogenic transcription factors (PPAR-γ and SREBP-1c) and multiple enzymes of the lipid biosynthesis pathways were down-regulated in the adipocytes (Table 2). Key lipogenic enzymes suppressed by protease inhibitors in adipocytes included FAS, glyceraldehyde-3-phosphate dehydrogenase, acyl-CoA ligases, hormone-sensitive lipase, hydroxysteroid dehydroge-

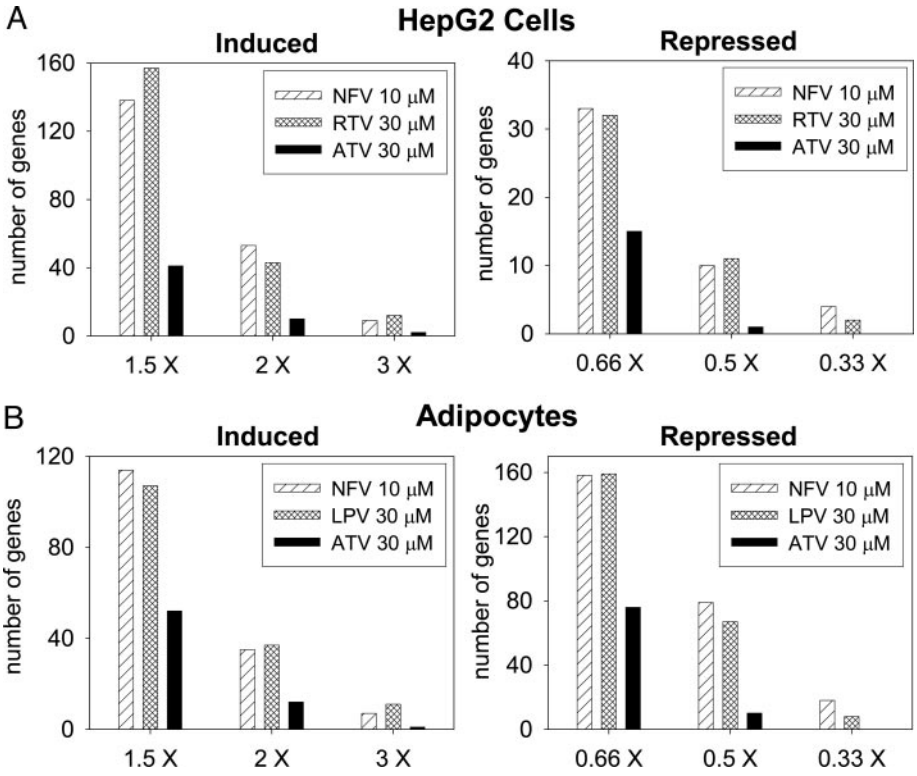

Fig. 3. Gene expression changes in protease inhibitor-treated versus control ($p < 0.01$) hepatocyte and adipocyte models using Affymetrix gene chips. Cells were treated for 24 h with protease inhibitors at the concentrations indicated, under conditions as per Fig. 2, A and E. A, for HepG2 cells, bars indicate the number of genes induced or repressed to the indicated extent among 22,214 RNA sequences assayed on Affymetrix U133A gene chips. B, for 3T3-L1 adipocytes, bars indicate the number of genes induced or repressed to the indicated extent among 12,422 sequences assayed on Affymetrix U74A-v2 gene chips. Drug abbreviations are as in Fig. 1.

TABLE 1

Transcriptional profile in protease inhibitor-treated HepG2 cells

HepG2 cells were treated with nelfinavir (3 and 10 μM), ritonavir (10 and 30 μM), or atazanavir (10 and 30 μM) for 24 h under the conditions used in the lipid synthesis assays. Cells were washed and RNA was isolated from triplicate cell incubations and gene expression profiles were conducted using the Affymetrix protocol. All genes with significant changes in expression for one or more of the treatments are included in the table. Data are expressed as mean mRNA concentration ratio of treated/control for treated/control for 30 μM atazanavir, 30 μM ritonavir, and 10 μM nelfinavir. Results are grouped by gene function.

Accession No.	Gene	30 μM Atazanavir	30 μM Ritonavir	10 μM Nelfinavir
Transcription factors				
NM_001675	ATF4	1.19	2.00*	2.27*
BC003600	CSRP3e, LIM-domain-only-4 (proteasome-interacting)	1.20	1.51*	2.07*
BC003637.1	GADD153 (C/EBP homologous protein)	1.03	1.49	1.88*
AL564683	C/EBP-β	1.17	1.36*	1.83*
NM_001806	C/EBP-γ	1.35	1.73*	1.75*
AI843895	SREBP-1c	1.08	1.33	1.48
ER stress response and signaling pathways				
AI435828	Stanniocalcin 2 (ER Ca^{2+} signaling, phosphate transport)	3.28*	6.09*	7.68*
NM_019058	RTP-801, hypoxia-inducible factor-responsive protein	1.32	2.57*	5.03*
BC005161	Activin βE	1.53	3.04*	4.12*
NM_021158	SINK neg regulator of nuclear factor-κB transactivator P65	1.27	2.81*	2.92*
NM_004362	Calmegin, ER chaperone, Ca^{2+} binding	1.27	1.77*	2.01*
NM_012328	HSP40, DnaJ homolog, subfamily B, member 9	1.39	3.03*	1.98*
BC002446.1	HSP40, DnaJ homolog, subfamily B, member 6	1.57*	2.00*	2.38*
BG403660	HSP105B	1.52	1.96*	1.98*
AA704004	HSP70, protein 8	1.19	1.49*	1.51
AF216292.1	BiP, GRP-78	1.11	1.36	1.06
NM_005080.1	X-box binding protein-1	0.89	1.18	0.99
NM_005627	Serum/glucocorticoid-regulated kinase	0.86	0.30*	0.21*
Amino acid and protein metabolism				
NM_001673	Asparagine synthetase	1.58	6.99*	7.79*
AB040875	Cystine/glutamate transporter	2.01*	6.89*	6.12*
AA488687	Expressed sequence tag	1.04	4.26*	4.70*
BE513104	Tyrosyl-tRNA synthetase	1.43*	3.33*	3.10*
NM_006636	Methylene-tetrahydrofolate dehydrogenase/cyclohydrolase	1.19	2.51*	2.77*
AL354872	Cystathionine γ-lyase	0.97	2.29*	2.59*
AB044548	Eukaryotic translation initiation factor 4E binding protein 1	1.38	2.85*	2.54*
NM_001751	Cysteinyl-tRNA synthetase	1.33	2.33*	2.49*
NM_006513	Seryl-tRNA synthetase	1.08	2.02*	2.35*
AI984005	Exportin T (nuclear export of tRNA)	1.01	2.46*	2.24*
BF340083	Glutamate/neutral amino acid transporter	1.21	2.22*	1.94*
NM_004990	Methionine tRNA synthetase	1.29	2.30*	2.27*
NM_021154	Phosphoserine aminotransferase	1.37*	2.48*	2.19*
NM_003191	Threonyl-tRNA synthetase	1.23	1.91*	2.02*
NM_005412	Serine hydroxymethyltransferase 2 (mitochondrial)	1.35*	2.47*	2.00*
NM_004446	Glutamyl-prolyl-tRNA synthetase	1.26	1.91*	1.96*
NM_013417	Isoleucine-tRNA synthetase	0.95	2.19*	1.94*
NM_000050	Argininosuccinate synthetase	1.31	1.88*	1.92*
NM_004184	Tryptophanyl-tRNA synthetase	1.19	2.11*	1.81*
AF217990	Homocys-inducible, ER stress-inducible, ubiquitin-like-1	1.35*	1.81*	1.68*
AF176699	Ubiquitin ligase	0.92	1.61*	1.41
NM_006398	Diubiquitin	0.74	0.41*	0.56*
Lipid metabolism				
BE855983	Acetyl-coenzyme A carboxylase-α	1.32	2.20	2.17*
NM_021122	Fatty acyl CoA ligase, long-chain 2	1.35	1.58*	1.82
NM_020299	Aldose reductase family 1, member 10	1.15	1.60*	1.70*
NM_001995	Fatty-acid-coenzyme A ligase, long-chain 1	1.29	1.52*	1.68*
NM_013389	NPC1	1.05	1.50*	1.63
AI189359	Mevalonate diphosphate decarboxylase	0.98	1.95*	1.61*
NM_012347	FAS	1.02	1.49*	1.61*
NM_012079	Diacylglycerol *O*-acyltransferase 1	1.73*	1.81*	1.60
NM_000786	Lanosterol 14-α-demethylase	1.03	1.81*	1.47*
NM_024090	Long-chain fatty acid elongase	1.12	1.54*	1.45*
NM_000527	Low-density lipoprotein receptor	0.90	1.40*	1.43*
AL136939	Long-chain polyunsaturated fatty acid elongation enzyme 2	1.13	1.50*	1.34
NM_001360	7-Deydrocholesterol reductase	1.11	1.90*	1.32
AL518627	3-Hydroxy-3-methylglutaryl-CoA reductase	1.01	1.53*	1.29
BE540552	Fatty acid desaturase 1	1.33	1.71*	1.23
AA639705	Squalene epoxidase	1.04	1.60*	1.07
Glucose and gluconeogenesis				
NM_004563	PEPCK	1.27	1.91*	2.04*
NM_001486	GKRP, glucokinase regulatory protein	1.23	1.58*	1.97
NM_006931	GLUT3	0.90	0.38*	0.35*
NM_000291	Phosphoglycerate kinase 1	1.03	0.79*	0.63*
NM_002654	Pyruvate kinase, M-type	0.98	0.68*	0.61*

* Significant differences from control, $p < 0.01$.

nase-1, and diacylglycerol *O*-acyltransferase 1. An exception to this pattern was the induction of the cholesterol trafficking protein NPC1 (also induced in HepG2 cells). The adipocytokines adiponectin and resistin were down-regulated, as was the intracellular cholesterol binding protein caveolin. Other metabolic enzymes suppressed in adipocytes included PEPCK and phosphofructokinase-bisphosphatase.

Time-course experiments in 3T3-L1 adipocytes using RT-PCR revealed rapid and strong induction of mRNA for GADD153 (to 6-fold with nelfinavir) and ATF3 (up to 35-fold with lopinavir), consistent with the ER stress response (Fig. 4B). The cholesterol trafficking gene NPC1 was also induced (to 5-fold with lopinavir). Atazanavir-treated cells were relatively unaffected. In agreement with the transcription profiles and lipid functional data, PCR assays showed time-dependent suppression of representative lipid and adipogenic genes in the adipocytes, with glyceraldehyde-3-phosphate dehydrogenase, FAS, and adiponectin reaching maximal suppression by 24 h (Fig. 4B). The time courses also exhibited a return of gene expression toward baseline levels at 32 h for both the ER stress and lipogenic genes, suggesting that the cells successfully mounted an effective counter-regulatory response to the effects of the protease inhibitors.

Discussion

The present studies add to a growing body of evidence directly linking the molecular pharmacology of HIV protease inhibitors to lipid and metabolic disturbances, including lipoatrophy, dyslipidemia, and insulin resistance. The marked down-regulation of lipogenic pathways in differentiated adipocytes contrasts with moderate up-regulation in hepatocytes, mirroring the clinical picture of lipoatrophy because of depletion of adipose triglyceride stores simultaneously with hepatic lipid overproduction and hyperlipidemia. The current findings help to integrate several mechanisms previously proposed for clinical side effects of protease inhibitors, including inhibition of glucose transport (Murata et al., 2000; Hruz et al., 2001; Hertel et al., 2004), suppression of adipocyte differentiation and lipogenesis (Dowell et al., 2000; Caron et al., 2003), and overproduction of lipids and disturbed apolipoprotein B processing by liver (Lenhard et al., 2000; Riddle et al., 2001; Hui, 2003). The data support an expanded role for the proteasome in linking ER stress responses with lipid and glucose regulation and membrane formation (Cox et al., 1997; Werstuck et al., 2001; Ozcan et al., 2004).

HIV protease inhibitors decreased proteasome chymotryptic activity and to a lesser extent tryptic activity in vitro at concentrations similar to the ranges that elicited gene expression and lipid functional effects in cells and inhibited glucose transport in adipocytes. These concentration dependencies are similar to the ranges of therapeutic plasma levels of protease inhibitors observed clinically (based on Physician's Desk Reference values). The data indicate that, relative to the high-affinity (nanomolar) proteasome inhibitors

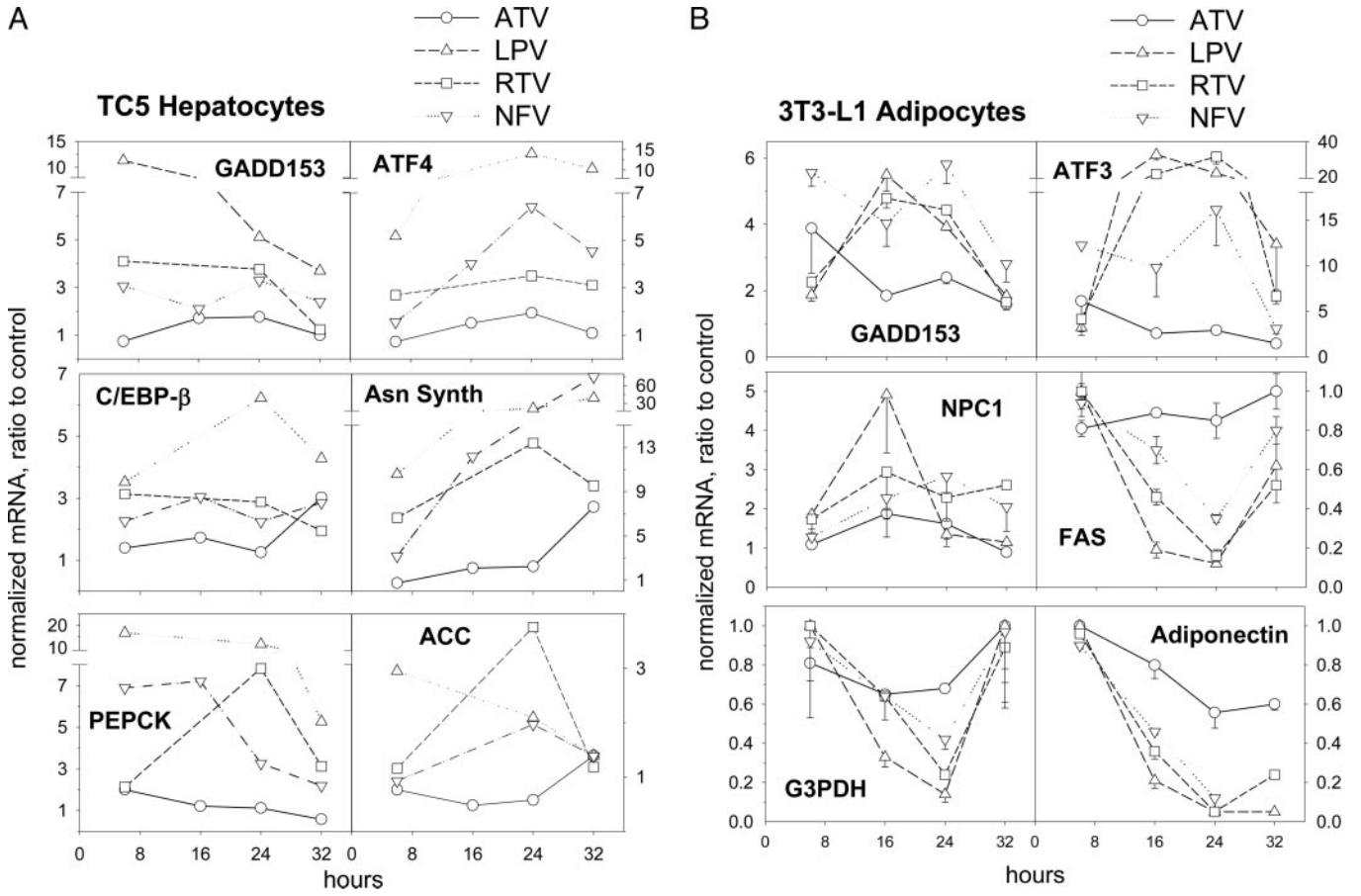

Fig. 4. Time dependence of mRNA regulatory responses to protease inhibitors in hepatocyte and adipocyte models assayed by PCR. A, mRNA changes in TC-5 hepatocyte cell line time course of protease inhibitor treatment. Mean values of triplicate samples assayed by RT-PCR are indicated as a function of cell incubation time. B, mRNA changes in 3T3-L1 adipocyte time course of protease inhibitor treatment. Mean values ± S.D. of two experiments each conducted in triplicate assayed by RT-PCR are indicated as a function of cell incubation time. Drug abbreviations are as in Fig. 1.

lactacystin and MG132, the HIV protease inhibitors are weak-to-moderate inhibitors of proteasome activity. The current results are consistent with previous reports that ritonavir and saquinavir inhibit chymotryptic activity of 20S proteasome in vitro and decrease protein degradation in cells (Schmidtke et al., 1999; Gaedicke et al., 2002; Pajonk et al., 2002). Our findings support the idea that protease inhibitors, nanomolar inhibitors of the HIV protease, are micromolar modulators of mammalian proteasome function and specificity, and at therapeutic levels can significantly affect processing and trafficking of specific proteins in the cell and trigger a counter-regulatory response.

Our observations are consistent with previous reports implicating interference by HIV protease inhibitors with processing of nuclear transcription factors SREBP-1 and -2, C/EBP-α, and PPAR-γ (Dowell et al., 2000; Caron et al., 2003; Hui, 2003). Proteolytic events control SREBP processing in the ER and Golgi as well the nucleus (Hirano et al., 2001). Nuclear turnover of SREBP was shown to be blocked by ritonavir in liver and adipose, leading to observed increases in nuclear SREBP levels (Riddle et al., 2001; Hui, 2003) These considerations support a broader role for proteasomal processing and degradation in cytoplasmic translocation, subnuclear localization, and coactivation of nuclear transcription factors. (Dino Rockel and von Mikecz, 2002; Nawaz and O'Malley, 2004).

Outside the nucleus, inhibition of proteasome activity in the ER and cytoplasm diminishes the efficient removal of

TABLE 2

Transcriptional profile in protease inhibitor-treated 3T3-L1 adipocytes

Differentiated 3T3-L1 cells were treated with protease inhibitors for 24 h under conditions used in the lipid synthesis assays. RNA from triplicate cell incubations was used for gene expression profiles conducted using Affymetrix protocols. All genes with significant changes in expression for one or more of the treatments are included in the table. Data are expressed as mean mRNA concentration ratio of treated/control for 30 μM atazanavir, 30 μM ritonavir, and nelfinavir 10 μM. Results are grouped by gene function.

Accession No.	Genes	30 μM Atazanavir	30 μM Lopinavir	10 μM Nelfinavir
Transcription factors				
U19118	ATF3	2.80	7.83*	4.17*
X67083	GADD153, C/EBP homologous protein-10	2.37	3.82*	3.93*
X51829	Myeloid differentiation primary response gene 116	2.41*	3.68*	3.33*
AI852641	Nuclear protein 1	2.17*	2.26*	2.62*
U00937	GADD45	1.80	2.88*	2.42*
X89749	TGIF, target gene interacting fact or	1.62	2.45*	2.16
M94087	ATF4	1.45*	1.46*	1.66*
U10374	PPAR-γ	0.67*	0.59*	0.56*
AI843895	SREBP-1c	0.76	0.63	0.78
M62362	C/EBP-α	0.76	0.48*	0.55*
AI834866	Nuclear receptor coactivator-4	0.74	0.60	0.58*
ER stress response and signaling pathways				
AI843119	Glutathione *S*-transferase ω 1	1.27	1.44*	1.72*
U53208	HSP40, DnaJ homolog, subfamily C, member 2	1.31	1.80*	1.51
L02914	Aquaporin-1	0.53	0.39	0.23*
AF077659	Homeodomain interacting protein kinase 2	0.64	0.37*	0.35*
Amino acid and protein metabolism				
U40930	Sequestosome 1 (binds ubiquitinylated proteins)	1.77*	2.65*	2.41*
U95053	Glutamate-cysteine ligase, regulatory subunit	1.39	2.16	1.94
AI851163	Tryptophanyl-tRNA synthetase	1.39	1.67*	1.78*
AI837395	Seryl-aminoacyl-tRNA synthetase 1	1.45	1.69*	1.60
AI839158	Proteasome 26S subunit-8	1.25	1.80*	1.25
AI836804	Proteasome subunit, α type 1	0.72	0.46*	0.41*
Lipid metabolism, adipogenesis				
AF003348	NPC1	1.68	3.27*	2.68*
AB033887	Fatty acyl-coenzyme A ligase, long chain 4	1.46	2.03*	2.36*
AA718169	Resistin	0.52*	0.31*	0.23*
Z48670	Peroxisomal fatty acyl-CoA transporter, ABC-D2	0.54	0.34	0.24*
U15977	Fatty acyl CoA ligase, long chain 2	0.54	0.31	0.27*
X72862	β-3 Adrenergic receptor	0.62	0.34*	0.30*
M61737	FSP27, fat-specific gene 27 kDa	0.67	0.31*	0.31*
M91458	Sterol carrier protein 2	0.67	0.31*	0.34*
X13135	FAS	0.61	0.39	0.38*
X95279	Spot14 gene (adipogenic marker, SREBP-regulated)	0.61*	0.35*	0.41*
AV290060	Glycerol phosphate dehydrogenase 1, cytoplasmic	0.63	0.42	0.45*
U37799	SRB1, scavenger receptor B1	0.74	0.48	0.44*
U69543	HSL, hormone sensitive lipase	0.75	0.36*	0.45*
X83202	Hydroxysteroid 11-β dehydrogenase 1	0.64*	0.49*	0.46*
AI747654	Caveolin, caveolae protein, 22 kDa	0.62*	0.46*	0.47*
AF045887	Angiotensinogen	0.76	0.58*	0.52*
M69260	Annexin A1	0.73	0.57	0.47*
U07159	Acyl-coenzyme A dehydrogenase, medium chain	0.73	0.56	0.53*
AF078752	Diacylglycerol acyltransferase 1	0.78	0.58*	0.53*
U49915	Adiponectin	0.73*	0.54*	0.57*
AF057368	7-Dehydrocholesterol reductase	0.88	0.60	0.53*
X04673	Adipsin	0.79	0.66*	0.69*
Glucose and gluconeogenesis				
X98848	6-Phosphofructo-2-kinase/fructose-2,6-biphosphatase 1	0.44	0.41	0.23*
AF009605	PEPCK	0.49	0.23*	0.28*
AF020039	Isocitrate dehydrogenase 1 ($NADP^+$), soluble	0.62*	0.51	0.45*
AI846739	Glycogen phosphorylase	0.67*	0.54*	0.50*

* Significant differences from control, $p < 0.01$.

misfolded nascent proteins, triggering the surveillance function of the UPR (Travers et al., 2000). The expression profiles in HepG2 cells and 3T3-L1 adipocytes reveal induction of the UPR signature genes ATF4, ATF3, GADD153, and GADD34. ATF4 and ATF3 are basic leucine zipper transcription factors that coregulate the eIF2 kinase stress pathway, leading to induction of GADD153 and the eukaryotic initiation factor 2α protein phosphatase regulatory subunit GADD34, ultimately providing feedback control and recovery from the UPR (Jiang et al., 2004). In our time-course data, gene expression trended back toward baseline at 32 h, suggesting an effective counter-regulatory response and recovery from the ER stress. The expression profiles for HIV protease inhibitor treated cells in our studies include several of the genes affected by the high-affinity proteasome inhibitors lactacystin and MG132 in human glioma cells, including ATF3 and GADD153 (Zimmermann et al., 2000). The up-regulation by HIV protease inhibitors of the DnaJ/HSP40 family of chaperone proteins in both the HepG2 and adipocyte profiles is consistent with the role of these proteins in regulating the ATPase activity and substrate binding of the chaperone Hsp70 in nascent protein processing (Shen et al., 2002). Although the interpretation of the present data relying largely on mRNA changes would be confirmed by assays of ER stress responses at the protein or biochemical level, the consistency of the transcriptional regulation observed leads to a strong conclusion of UPR and ER stress response under the conditions of the experiments.

The induction of amino acid synthetic enzymes, transporters, and amino acyl-tRNA synthetases as seen in our expression profiles suggests signaling through decreased intracellular amino acid and amino acyl-tRNA pools. Other studies have demonstrated that glucose as well as amino acid deprivation up-regulates nutrient responsive genes such as asparagine synthetase. This is mediated by ATF4 and C/EBP-β induction and activation of their target gene promoter nutrient-response elements, while increasing ATF3 expression serves to counter-regulate these target genes (Siu et al., 2002; Pan et al., 2003). It is interesting that asparagine synthetase was highly induced by protease inhibitors in HepG2 cells, which also exhibited significant elevations in ATF4 and C/EBP-β but not ATF3. In contrast, adipocytes expressed higher ATF3 than ATF4 and did not increase asparagine synthetase expression in our profiles. Consistent with a role for ATF4 in HepG2 cell responses, we also observed high induction of stanniocalcin-2 by protease inhibitors, a gene recently described as a target of ATF4 induction in the UPR (Ito et al., 2004).

Several clinical studies suggest that lipoatrophy of peripheral/subcutaneous adipose tissues is a major feature of the HIV-associated lipodystrophy syndrome and of the use of protease inhibitors (Carr, 2000). The use of nucleoside reverse transcriptase inhibitors is also associated with lipoatrophy (Nolan and Mallal, 2004), and it has been proposed that the combination of this class with protease inhibitors may amplify this component of the syndrome. Although it is nearly impossible to fully separate the effects of the drug classes in the clinical data, animal models have demonstrated lipoatrophy in protease inhibitor-treated mice (Goetzman et al., 2003) as well hypertriglyceridemia and liver and adipose SREBP pathway disturbances in mice (Riddle et al., 2001). It is possible that subcutaneous fat may be more sensitive than central fat depots to diminished expression of PPAR-γ and other changes in gene expression that we and others have observed with protease inhibitors. Because insulin profoundly inhibits lipolysis in adipocytes, the effects of protease inhibitors on insulin resistance could also contribute to lipolysis and diminished fat storage seen in lipoatrophy.

In summary, our findings of protease inhibitor-specific effects on gene expression and lipid and glucose metabolism in in vitro models are consistent with emerging reports of clinical trials that describe metabolic and lipid profiles after treatment with the various agents (Cahn et al., 2004; Wood et al., 2004; Johnson, 2005). Future studies directed toward the comparative profiles of the different members of the protease inhibitor class may help address whether the in vitro properties are predictive of human clinical findings. The effects observed in the present studies on glucose transporter activity (particularly GLUT4) in adipocytes are consistent with recent reports showing differential effects on glucose disposal in human subjects studied by euglycemic hyperinsulinemic clamp technique (Noor et al., 2002, 2004). The dysregulation of lipogenesis and the ER stress responses in liver and adipocyte cellular models was seen at concentrations near or below respective therapeutic plasma levels in patients, suggesting that they could be related to the clinical lipid profiles of the protease inhibitors (Haas et al., 2003; Murphy et al., 2003; Sanne et al., 2003; Calza et al., 2004; Squires et al., 2004). Although controlled long term data on changes in body fat distribution are not yet available, it is interesting to note that peripheral fat loss and lipodystrophy have not been observed on atazanavir-containing HAART regimens at up to 48-week treatment (Haerter et al., 2004).

Finally, the data suggest several candidate genes and pathways as targets for further exploration in genotyping and pharmacogenomic analysis of susceptibility to dyslipidemia, lipodystrophy, and related metabolic disturbances in HIV. Together with work by others, our findings support a unifying hypothesis that protease inhibitors induce ER stress through proteasome inhibition, resulting in contrasting effects on lipogenic pathways in adipocytes and hepatocytes depending on the cell-specific degree of glucose transport inhibition. Together, these processes would contribute to excessive hepatic lipid production but diminished storage of fat in peripheral subcutaneous adipose tissue and may explain clinical observations of dyslipidemia, insulin resistance, and fat redistribution.

References

Cahn PE, Gatell JM, Squires K, Percival LD, Piliero PJ, Sanne IA, Shelton S, Lazzarin A, Odeshoo L, Kelleher TD, et al. (2004) Atazanavir–a once-daily HIV protease inhibitor that does not cause dyslipidemia in newly treated patients: results from two randomized clinical trials. *J Int Assoc Physicians AIDS Care (Chic Ill)* **3:**92–98.

Calza L, Manfredi R, and Chiodo F (2004) Dyslipidaemia associated with antiretroviral therapy in HIV-infected patients. *J Antimicrob Chemother* **53:**10–14.

Caron M, Auclair M, Sterlingot H, Kornprobst M, and Capeau J (2003) Some HIV protease inhibitors alter lamin A/C maturation and stability, SREBP-1 nuclear localization and adipocyte differentiation. *AIDS* **17:**2437–2444.

Carr A (2000) HIV protease inhibitor-related lipodystrophy syndrome. *Clin Infect Dis* **30 (Suppl 2):**S135–S142.

Cox JS, Chapman RE, and Walter P (1997) The unfolded protein response coordinates the production of endoplasmic reticulum protein and endoplasmic reticulum membrane. *Mol Biol Cell* **8:**1805–1814.

Dino Rockel T and von Mikecz A (2002) Proteasome-dependent processing of nuclear proteins is correlated with their subnuclear localization. *J Struct Biol* **140:**189–199.

Dowell P, Flexner C, Kwiterovich PO, and Lane MD (2000) Suppression of preadipocyte differentiation and promotion of adipocyte death by HIV protease inhibitors. *J Biol Chem* **275:**41325–41332.

Gaedicke S, Firat-Geier E, Constantiniu O, Lucchiari-Hartz M, Freudenberg M, Galanos C, and Niedermann G (2002) Antitumor effect of the human immunodeficiency virus protease inhibitor ritonavir: induction of tumor-cell apoptosis associated with perturbation of proteasomal proteolysis. *Cancer Res* **62:**6901–6908.
Goetzman ES, Tian L, Nagy TR, Gower BA, Schoeb TR, Elgavish A, Acosta EP, Saag MS, and Wood PA (2003) HIV protease inhibitor ritonavir induces lipoatrophy in male mice. *AIDS Res Hum Retroviruses* **19:**1141–1150.
Haas DW, Zala C, Schrader S, Piliero P, Jaeger H, Nunes D, Thiry A, Schnittman S, and Sension M (2003) Therapy with atazanavir plus saquinavir in patients failing highly active antiretroviral therapy: a randomized comparative pilot trial. *AIDS* **17:**1339–1349.
Haerter G, Manfras B, Mueller M, Kern P, and Trein A (2004) Regression of lipodystrophy in HIV-infected patients under therapy with the new protease inhibitor atazanavir. *AIDS* **18:**952–955.
Hertel J, Struthers H, Horj CB, and Hruz PW (2004) A structural basis for the acute effects of HIV protease inhibitors on GLUT4 intrinsic activity. *J Biol Chem* **279:**55147–55152.
Hirano Y, Yoshida M, Shimizu M, and Sato R (2001) Direct demonstration of rapid degradation of nuclear sterol regulatory element-binding proteins by the ubiquitin-proteasome pathway. *J Biol Chem* **276:**36431–36437.
Hruz PW, Murata H, and Mueckler M (2001) Adverse metabolic consequences of HIV protease inhibitor therapy: the search for a central mechanism. *Am J Physiol* **280:**E549–E553.
Hui DY (2003) Effects of HIV protease inhibitor therapy on lipid metabolism. *Prog Lipid Res* **42:**81–92.
Ito D, Walker JR, Thompson CS, Moroz I, Lin W, Veselits ML, Hakim AM, Fienberg AA, and Thinakaran G (2004) Characterization of stanniocalcin 2, a novel target of the mammalian unfolded protein response with cytoprotective properties. *Mol Cell Biol* **24:**9456–9469.
Jiang HY, Wek SA, McGrath BC, Lu D, Hai T, Harding HP, Wang X, Ron D, Cavener DR, and Wek RC (2004) Activating transcription factor 3 is integral to the eukaryotic initiation factor 2 kinase stress response. *Mol Cell Biol* **24:**1365–1377.
Johnson N (2005) Atazanavir, with ritonavir or saquinavir and lopinavir/ritonavir in patients experiencing multiple virological failures. *AIDS* **19:**153–162.
Kaufman RJ, Scheuner D, Schroder M, Shen X, Lee K, Liu CY, and Arnold SM (2002) The unfolded protein response in nutrient sensing and differentiation. *Nat Rev Mol Cell Biol* **3:**411–421.
Lenhard JM, Croom DK, Weiel JE, and Winegar DA (2000) HIV protease inhibitors stimulate hepatic triglyceride synthesis. *Arterioscler Thromb Vasc Biol* **20:**2625–2629.
Liang JS, Distler O, Cooper DA, Jamil H, Deckelbaum RJ, Ginsberg HN, and Sturley SL (2001) HIV protease inhibitors protect apolipoprotein B from degradation by the proteasome: a potential mechanism for protease inhibitor-induced hyperlipidemia. *Nat Med* **7:**1327–1331.
Murata H, Hruz PW, and Mueckler M (2000) The mechanism of insulin resistance caused by HIV protease inhibitor therapy. *J Biol Chem* **275:**20251–20254.
Murphy RL, Sanne I, Cahn P, Phanuphak P, Percival L, Kelleher T, and Giordano M (2003) Dose-ranging, randomized, clinical trial of atazanavir with lamivudine and stavudine in antiretroviral-naive subjects: 48-week results. *AIDS* **17:**2603–2614.
Nawaz Z and O'Malley BW (2004) Urban renewal in the nucleus: is protein turnover by proteasomes absolutely required for nuclear receptor-regulated transcription? *Mol Endocrinol* **18:**493–499.
Nolan D and Mallal S (2004) The role of nucleoside reverse transcriptase inhibitors in the fat redistribution syndrome. *J HIV Ther* **9:**34–40.
Noor MA, Parker RA, O'Mara E, Grasela DM, Currie A, Hodder SL, Fiedorek FT, and Haas DW (2004) The effects of HIV protease inhibitors atazanavir and lopinavir/ritonavir on insulin sensitivity in HIV-seronegative healthy adults. *AIDS* **18:**2137–2144.
Noor MA, Seneviratne T, Aweeka FT, Lo JC, Schwarz JM, Mulligan K, Schambelan M, and Grunfeld C (2002) Indinavir acutely inhibits insulin-stimulated glucose disposal in humans: a randomized, placebo-controlled study. *AIDS* **16:**F1–F8.
Ozcan U, Cao Q, Yilmaz E, Lee AH, Iwakoshi NN, Ozdelen E, Tuncman G, Gorgun C, Glimcher LH, and Hotamisligil GS (2004) Endoplasmic reticulum stress links obesity, insulin action and type 2 diabetes. *Science (Wash DC)* **306:**457–461.
Pajonk F, Himmelsbach J, Riess K, Sommer A, and McBride WH (2002) The human immunodeficiency virus (HIV)-1 protease inhibitor saquinavir inhibits proteasome function and causes apoptosis and radiosensitization in non-HIV-associated human cancer cells. *Cancer Res* **62:**5230–5235.
Pan Y, Chen H, Siu F, and Kilberg MS (2003) Amino acid deprivation and endoplasmic reticulum stress induce expression of multiple activating transcription factor-3 mRNA species that, when overexpressed in HepG2 cells, modulate transcription by the human asparagine synthetase promoter. *J Biol Chem* **278:**38402–38412.
Parker R, Wang S, Mulvey R, Fenderson W, Elosua C, Laing N, Yang W-P, and Flint O (2003) Proteasome and glucose transport inhibition: a unifying hypothesis for the mechanism of protease inhibitor-induced metabolic disturbances and for the superior lipid profile of atazanavir. *Antivir Ther* **8:**S380.
Purnell JQ, Zambon A, Knopp RH, Pizzuti DJ, Achari R, Leonard JM, Locke C, and Brunzell JD (2000) Effect of ritonavir on lipids and post-heparin lipase activities in normal subjects. *AIDS* **14:**51–57.
Riddle TM, Kuhel DG, Woollett LA, Fichtenbaum CJ, and Hui DY (2001) HIV protease inhibitor induces fatty acid and sterol biosynthesis in liver and adipose tissues due to the accumulation of activated sterol regulatory element-binding proteins in the nucleus. *J Biol Chem* **276:**37514–37519.
Rodgers KJ and Dean RT (2003) Assessment of proteasome activity in cell lysates and tissue homogenates using peptide substrates. *Int J Biochem Cell Biol* **35:**716–727.
Sanne I, Piliero P, Squires K, Thiry A, and Schnittman S (2003) Results of a phase 2 clinical trial at 48 weeks (AI424-007): a dose-ranging, safety and efficacy comparative trial of atazanavir at three doses in combination with didanosine and stavudine in antiretroviral-naive subjects. *J Acquir Immune Defic Syndr* **32:**18–29.
Schmidtke G, Holzhutter HG, Bogyo M, Kairies N, Groll M, de Giuli R, Emch S, and Groettrup M (1999) How an inhibitor of the HIV-I protease modulates proteasome activity. *J Biol Chem* **274:**35734–35740.
Shen Y, Meunier L, and Hendershot LM (2002) Identification and characterization of a novel endoplasmic reticulum (ER) DnaJ homologue, which stimulates ATPase activity of BiP in vitro and is induced by ER stress. *J Biol Chem* **277:**15947–15956.
Siu F, Bain PJ, LeBlanc-Chaffin R, Chen H, and Kilberg MS (2002) ATF4 is a mediator of the nutrient-sensing response pathway that activates the human asparagine synthetase gene. *J Biol Chem* **277:**24120–24127.
Squires K, Lazzarin A, Gatell JM, Powderly WG, Pokrovskiy V, Delfraissy JF, Jemsek J, Rivero A, Rozenbaum W, Schrader S, et al. (2004) Comparison of once-daily atazanavir with efavirenz, each in combination with fixed-dose zidovudine and lamivudine, as initial therapy for patients infected with HIV. *J Acquir Immune Defic Syndr* **36:**1011–1019.
Travers KJ, Patil CK, Wodicka L, Lockhart DJ, Weissman JS, and Walter P (2000) Functional and genomic analyses reveal an essential coordination between the unfolded protein response and ER-associated degradation. *Cell* **101:**249–258.
Werstuck GH, Lentz SR, Dayal S, Hossain GS, Sood SK, Shi YY, Zhou J, Maeda N, Krisans SK, Malinow MR, et al. (2001) Homocysteine-induced endoplasmic reticulum stress causes dysregulation of the cholesterol and triglyceride biosynthetic pathways. *J Clin Investig* **107:**1263–1273.
Woerle HJ, Mariuz PR, Meyer C, Reichman RC, Popa EM, Dostou JM, Welle SL, and Gerich JE (2003) Mechanisms for the deterioration in glucose tolerance associated with HIV protease inhibitor regimens. *Diabetes* **52:**918–925.
Wood R, Phanuphak P, Cahn P, Pokrovskiy V, Rozenbaum W, Pantaleo G, Sension M, Murphy R, Mancini M, Kelleher T, et al. (2004) Long-term efficacy and safety of atazanavir with stavudine and lamivudine in patients previously treated with nelfinavir or atazanavir. *J Acquir Immune Defic Syndr* **36:**684–692.
Zimmermann J, Erdmann D, Lalande I, Grossenbacher R, Noorani M, and Furst P (2000) Proteasome inhibitor induced gene expression profiles reveal overexpression of transcriptional regulators ATF3, GADD153 and MAD1. *Oncogene* **19:**2913–2920.

Address correspondence to: Dr. Rex A. Parker, Metabolic and Cardiovascular Discovery Biology, Bristol-Myers Squibb Pharmaceutical Research Institute, 311 Pennington-Rocky Hill Rd., Pennington, NJ 08534. E-mail: rex.parker@bms.com